Supporting Information

An easy and smart way to explore the light-emitting responses of carbon dot and doxorubicin hydrochloride assembly: white light generation and pH-dependent reversible photoswitching

Arghajit Pyne, Souvik Layek, Avijit Patra and Nilmoni Sarkar*

Department of Chemistry, Indian Institute of Technology, Kharagpur 721302, WB, India

***Corresponding Author: Nilmoni Sarkar**

E-mail: nilmoni@chem.iitkgp.ac.in; nilmonisarkar1208@gmail.com

Fax: 91-3222-255303

1. Detailed Instrumentation

1.1. Fourier transform infrared (FTIR) measurement

We used Nexus 870 FTIR spectrometer to record the fourier transform infrared (FTIR) spectrum of the sample presented in the manuscript in the range of 500−4000 cm^{-1}. The sample was recorded with 32 scans at a spectral resolution of 1.928 cm^{-1}. Furthermore, we employed the OMNIC software (version-6.0) of the Thermo Nicolet Corporation for the spectral analysis. All the measurements were performed at room temperature (25 °C).

1.2. Thermogravimetric (TGA) analysis

We performed the thermogravimetric analysis (TGA) employing the NETZSCH TG209 F3 Tarsus instrument. The study was carried out under N_2 atmosphere, ranging from room temperature to 800 °C with a heating rate of 10 K/min.

1.3. UV-visible absorption and steady state emission studies

UV-visible absorption study was performed using a Shimadzu (model number UV 2450) spectrophotometer while for steady state emission measurements, we employed a Shimadzu (RF-6000) spectrofluorimeter (or spectrofluorometer or spectrofluorophotometer). The CD samples were mostly excited at 400 nm, otherwise specified. The steady state excitation spectra were also recorded in the same instrument.

1.4. Time resolved fluorescence (TCSPC) measurements

In this present manuscript, all the time resolved fluorescence measurements were addressed employing the time correlated single photon counting (Deltaflex TCSPC) instrument in the forward mode. The instrumentation comprised of a picosecond diode laser of 405 nm as the excitation light source along with a PPD detector to detect the signal in magic angle (54.7°) polarization. For our TCSPC setup, the typical instrument response function was ~210 ps. The EzTime decay analysis software was used for the analysis of the collected decays. The average lifetime was obtained from the same software which uses the following equation,

$$\tau_{\text{average}} = a_1 \tau_{1+} a_2 \tau_{2+} a_3 \tau_3$$

Where, τ_is are the lifetime components in nanoseconds (ns), a_is are respective normalized contributions and $\sum a_i = 1$. The average lifetime is indicated by τ_{average} or τ_{avg}.

The detailed instrumental description for the used TCSPC setup was discussed in our earlier publications[S1,S2]. However, in all the TCSPC decay traces throughout our manuscript, the y-axis is designated as intensity which is actually counts in logarithmic scale (i.e. counts (log)).

1.5. Dynamic light scattering (DLS) and zeta potential (ξ) measurements

The dynamic light scattering (DLS) measurement was performed to get a qualitative idea about the size of the CD system. A Malvern Nano ZS instrument employing a 4 mW He−Ne laser (λ = 632.8 nm) and equipped with a thermostated sample chamber was used for the measurement. Nevertheless, the DLS measurement is very much useful for the size determination of the spherical and near spherical aggregates, whereas for nonspherical aggregates it may produce erroneous results. Moreover, the zeta potential (ζ) measurement was also performed in the same instrument with the detector positioned at 173° angle.

1.6. High resolution transmission electron microscopy (HR-TEM) measurement

High resolution transmission electron microscopy (HR-TEM) measurement is a well known microscopic technique which gives direct morphological scenario of different molecular architectures. This HR-TEM measurement was carried out using a JEOL Model JEM-2100 instrument operating at 200 kV acceleration voltage. For HR-TEM measurements, the as prepared sample (about 10 μl of the sample) was placed on the carbon-coated (50 nm carbon film) Cu grid (300 mesh, Electron Microscopy Science) and allowed to dry overnight prior to the experiments.

1.7. Atomic force microscopy (AFM) measurement

The other microscopy based morphological characterization technique, atomic force microscopy (AFM) image was recorded using the Agilent 5500 instrument in the tapping mode. The sample preparation for this measurement was similar to the other microscopic technique i.e. HR-TEM. Briefly, a drop of very dilute sample solution (~ 1000 times dilute of the stock solution) was drop casted on a clean glass surface and completely dried for 24 h prior to the measurement.

1.8. Powder x-ray diffraction (XRD) study

The powder x-ray diffreaction (XRD) study was recorded with a Bruker D8-advance diffractometer at room temperature (25°C). The sample was provided in dry powder form and scanned within the range of 2θ from 10 to 70°.

2. Supporting Table

Table S1. The stretching vibrational frequencies and corresponding functional groups responsible for synthesized CD[a]

FTIR Stretching Frequency	Responsible Functional Group(s)
3455 cm^{-1}	-OH and $-NH_2$
1635 cm^{-1}	C=O of amide and or C=N
1470 cm^{-1}	C=C
1370 cm^{-1}	C-N
1050 and 1120 cm^{-1}	C-O and C-O-C epoxy

[a]Experimental error ±5%

Table S2. Comparison between uv-visible absorption spectra and steady state excitation spectra

UV-vis absorption spectra	Steady state excitation spectra
280 nm	278 nm
338 nm	332 nm
392 nm	375-390 nm
440 nm	440 nm

Table S3. Fitted lifetime values for dialyzed CD solution at different emission points[b]

Emission Wavelength	τ_1 (a_1) (ns)	τ_2 (a_2) (ns)	τ_3 (a_3) (ns)	τ_{avg} (ns)	χ^2
435 nm	0.77 (0.44)	4.18 (0.28)	10.88 (0.28)	4.58	1.13
455 nm	0.33 (0.50)	2.77 (0.26)	9.9 (0.24)	3.26	1.19
477 nm	0.5 (0.49)	3.26 (0.27)	9.53 (0.24)	3.38	1.10
495 nm	0.43 (0.47)	3.05 (0.28)	8.91 (0.25)	3.28	1.19
515 nm	0.32 (0.54)	2.93 (0.26)	8.47 (0.20)	2.63	1.09
525 nm	0.38 (0.55)	2.73 (0.23)	7.75 (0.22)	2.53	1.18
535 nm	0.42 (0.53)	3.04 (0.26)	7.9 (0.21)	2.72	1.07
555 nm	0.34 (0.60)	2.66 (0.22)	7.52 (0.18)	2.18	1.09

[b]**Experimental error in lifetime values ±5%**

Table S4. Fitted lifetime values for the pH effect of the dialyzed CD solution[c]

System	Emission Wavelength	τ_1 (a_1) (ns)	τ_2 (a_2) (ns)	τ_3 (a_3) (ns)	τ_{avg} (ns)	χ^2
CD	495 nm	0.43 (0.47)	3.05 (0.28)	8.91 (0.25)	3.28	1.19
CD@ pH 2	525 nm	0.42 (0.53)	2.26 (0.35)	6.14 (0.12)	1.76	1.08
CD@ pH 12	477 nm	0.36 (0.51)	3.12 (0.25)	9.83 (0.24)	3.27	1.16

[c]**Experimental error in lifetime values ±5%**

Table S5. Fitted lifetime values for the pH reversibility of the dialyzed CD solution[d]

System	Emission Wavelength	τ_1 (a_1) (ns)	τ_2 (a_2) (ns)	τ_3 (a_3) (ns)	τ_{avg} (ns)	χ^2
CD@ pH 12-C1	477 nm	0.36 (0.51)	3.12 (0.25)	9.83 (0.24)	3.27	1.16
CD@ pH 2-C1	471 nm	0.39 (0.49)	2.23 (0.33)	5.85 (0.18)	1.99	1.22
CD@ pH 12-C2	477 nm	0.36 (0.56)	3.21 (0.22)	9.95 (0.22)	3.14	1.08
CD@ pH 2-C2	471 nm	0.34 (0.47)	1.98 (0.32)	5.47 (0.21)	1.93	1.09
CD@ pH 12-C3	477 nm	0.38 (0.57)	3.09 (0.21)	9.85 (0.22)	3.04	1.09
CD@ pH 2-C3	471 nm	0.38 (0.51)	2.28 (0.34)	6.11 (0.15)	1.86	1.13
CD@ pH 12-C4	477 nm	0.46 (0.49)	3.31 (0.25)	9.98 (0.26)	3.68	1.13
CD@ pH 2-C4	471 nm	0.35 (0.51)	2.19 (0.3)	6.01 (0.19)	1.96	1.13

[d]Experimental error in lifetime values ±5%

Table S6. Table for CIE coordinates of the excitation dependency of CD-Dox WL system. The bracketed excitation wavelength produced WL emission of the system.

CD-Dox WL System @ Varying Excitation Wavelengths (nm)	CIE Coordinates (x,y)
300	(0.28, 0.44)
330	(0.28, 0.28)
350	(0.27, 0.27)
375	(0.27, 0.28)
395	(0.30, 0.32)
400	(0.32, 0.34)
405	(0.36, 0.37)
420	(0.46, 0.45)
440	(0.51, 0.47)

Table S7. Fitted lifetime values of probable FRET between CD and Dox for WL generation[e]

System	Emission Wavelength	τ_1 (a_1) (ns)	τ_2 (a_2) (ns)	τ_3 (a_3) (ns)	τ_{avg} (ns)	χ^2
CD@ pH 12	477 nm	0.46 (0.49)	3.31 (0.25)	9.98 (0.26)	3.68	1.13
CD@ pH 2 (i.e. CD @ pH 12+HCl)	471 nm	0.39 (0.49)	2.23 (0.33)	5.85 (0.18)	1.99	1.22
CD@ pH 2 +Dox_WL	471 nm	0.47 (0.51)	2.59 (0.33)	6.59 (0.16)	2.15	1.09
CD@ pH 2 +Dox_WL	592 nm	0.34 (0.20)	1.06 (0.73)	4.78 (0.07)	1.15	1.19
Dox@ pH 2	592 nm	1.01 (1.00)	-	-	1.01	1.23

[e]Experimental error in lifetime values ±5%

Table S8. Table for the reversibility of the CIE coordinates and CRI values for the pH mediated reversible photoswitching of the CD-Dox WL system

Sample Description		CIE Coordinates (x,y)	CRI Values
WL ON@ pH 2	Cycle 1	(0.32, 0.34)	88
	Cycle 2	(0.32, 0.34)	88
	Cycle 3	(0.32, 0.34)	88
	Cycle 4	(0.32, 0.34)	88
WL OFF@ pH 12	Cycle 1	(0.20, 0.27)	-
	Cycle 2	(0.20, 0.27)	-
	Cycle 3	(0.20, 0.27)	-

Table S9. Fitted lifetime values for pH dependent reversible photoswitching of CD-Dox WL[f]

System	Emission Wavelength	τ_1 (a_1) (ns)	τ_2 (a_2) (ns)	τ_3 (a_3) (ns)	τ_{avg} (ns)	χ^2
WL-ON@ pH 2-C1	471 nm	0.34 (0.49)	1.94 (0.28)	5.63 (0.23)	2.00	1.07
WL-OFF@ pH 12-C1	471 nm	0.31 (0.55)	2.85 (0.22)	9.69 (0.23)	3.03	1.1
WL-ON@ pH 2-C2	471 nm	0.25 (0.54)	1.9 (0.31)	5.58 (0.15)	1.56	1.13
WL-OFF@ pH 12-C2	471 nm	0.29 (0.58)	2.77 (0.2)	9.63 (0.22)	2.8	1.18
WL-ON@ pH 2-C3	471 nm	0.28 (0.54)	1.8 (0.35)	5.91 (0.11)	1.45	1.26
WL-OFF@ pH 12-C3	471 nm	0.30 (0.59)	2.89 (0.20)	9.7 (0.21)	2.81	1.1
WL-ON@ pH 2-C4	471 nm	0.28 (0.56)	1.75 (0.34)	6.06 (0.10)	1.38	1.12

[f]Experimental error in lifetime values ±5%

Table S10. Stepwise truth tables of LOGIC GATEs for (a) generation and (b) pH mediated reversible photoswitching of CD-Dox WL

(a)

CD@pH 12 (Input 1)	Dox (Input 2)	Output 1 (i.e. WL)
0	0	0
0	1	0
1	0	0
1	1	0

NO GATE

Output 1	pH 2 (i.e. HCl) (Input 3)	Output 2 (i.e. WL)
0	0	0
0	1	0
1	0	0
1	1	1

AND GATE

(b)

WL (Input 5)	pH 12 (i.e. NaOH) (Input 6)	Output 3 (i.e. WL)
0	0	0
0	1	0
1	0	1
1	1	0

INHIBITION GATE

Output 3	pH 2 (i.e. HCl) (Input 7)	Output 4 (i.e. WL)
0	0	0
0	1	0
1	0	0
1	1	1

AND GATE

3. Supporting Figures.

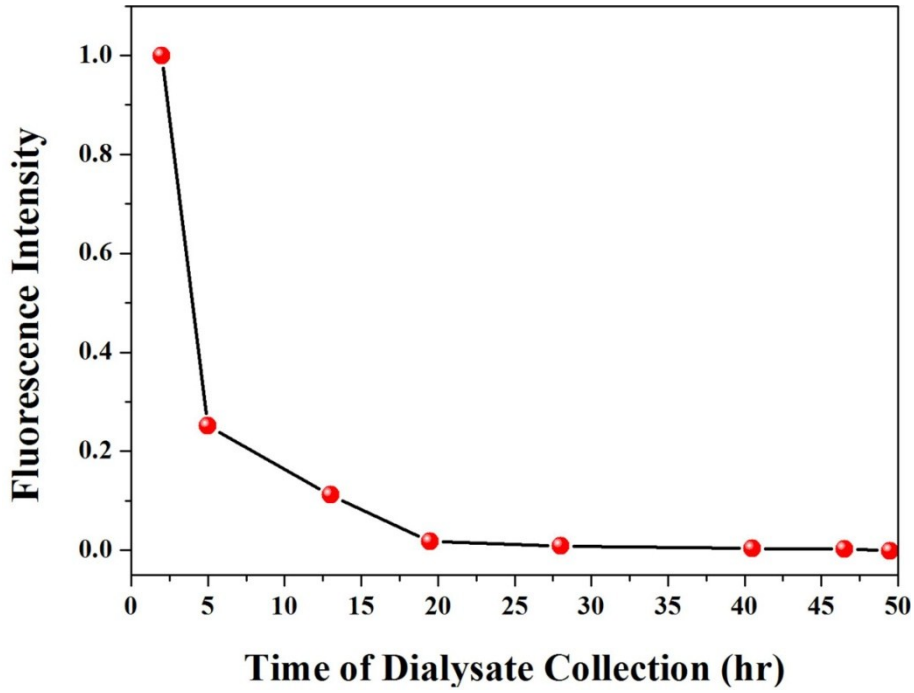

Figure S1. Steady state emission intensities of the collected dialysate (solution outside the dialysis bag) fractions. The time in the x-axis indicates the time interval after which dialysate was collected and replaced by fresh water. The plot indicates that at 50 h, the emission intensity of the dialysate is almost zero i.e. the dialysis process was complete.

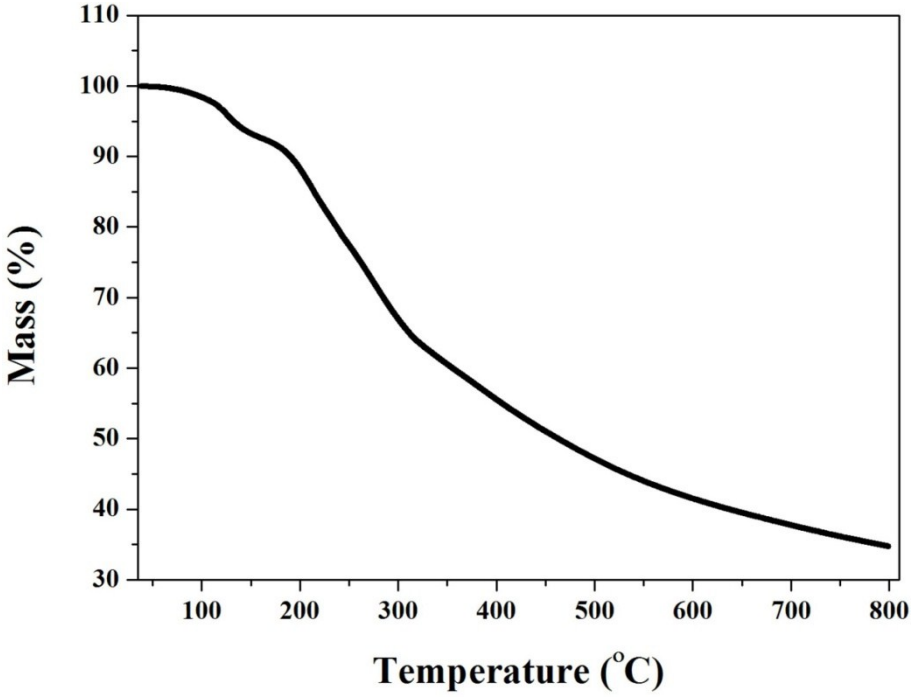

Figure S2. Thermogravimetric analysis (TGA) curve for synthesized CD powder. The plot indicates that the synthesized CD was stable up to ~240 °C (~ 80% residual mass).

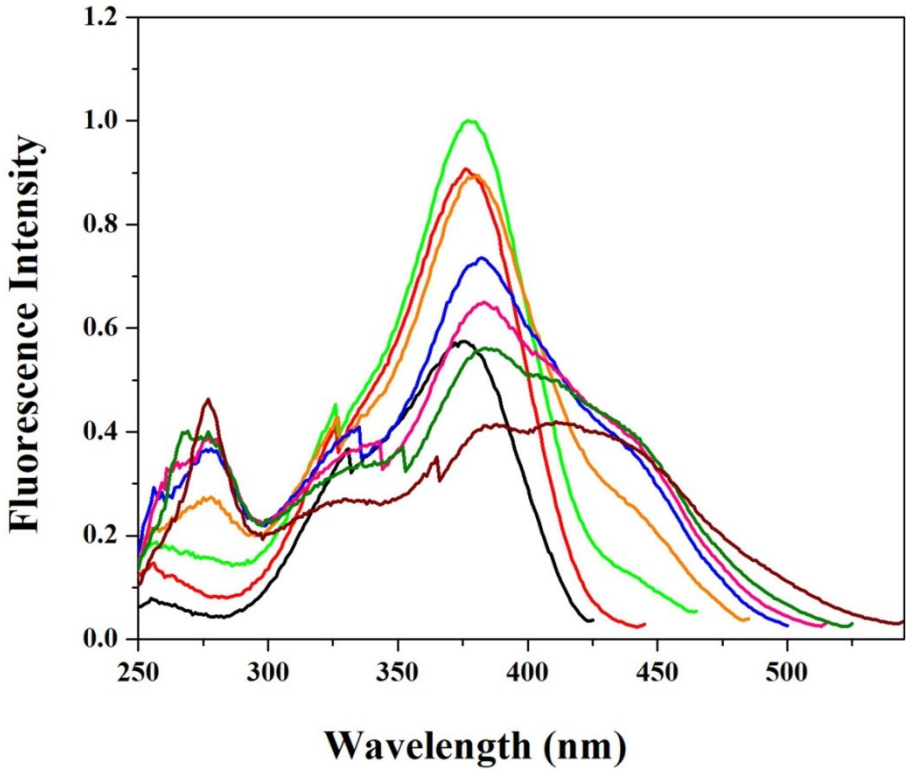

Figure S3. Steady state excitation spectra of the dialyzed CD solution for 435 (black curve), 455 (red curve), 475 (green curve), 495 (orange curve), 515 (blue curve), 535 (pink curve) and 555 (wine curve) nm emission wavelengths.

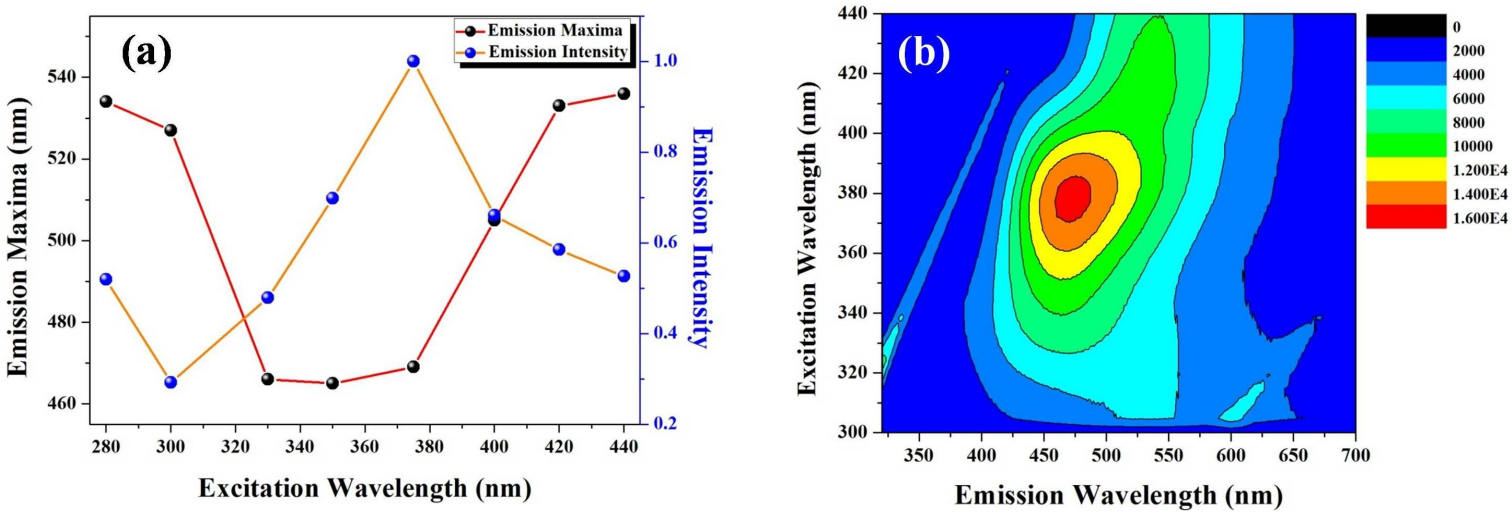

Figure S4. (a) 2-D and (b) 3-D excitation-emission map of the dialyzed CD solution.

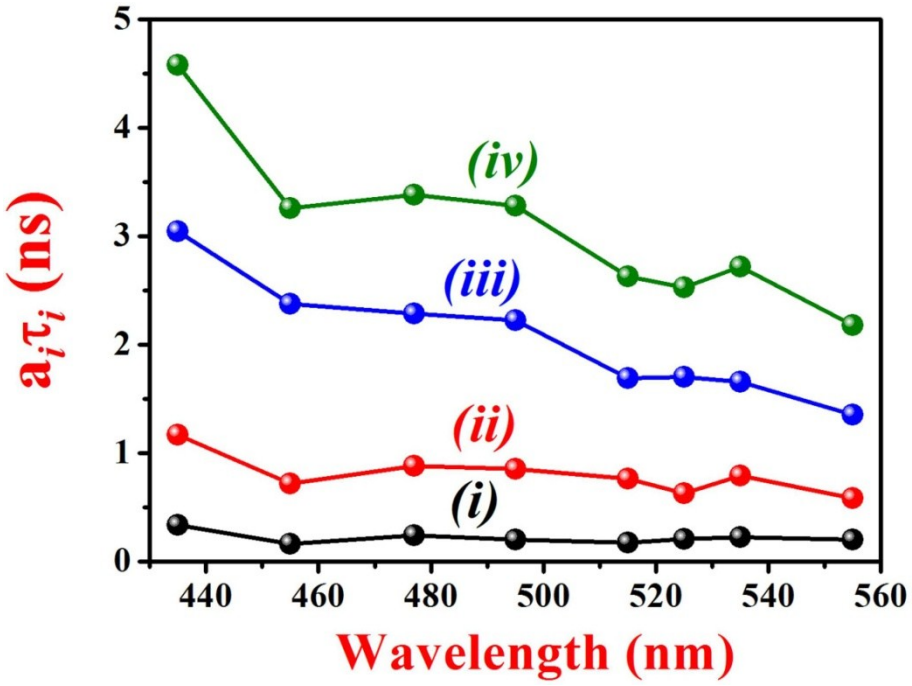

Figure S5. Variation of fitted TCSPC decay parameters with emission wavelengths; (i), (ii), (iii) and (iv) indicate $a_1\tau_1$, $a_2\tau_2$, $a_3\tau_3$ and $\tau_{average}$ vs emission wavelength plots respectively.

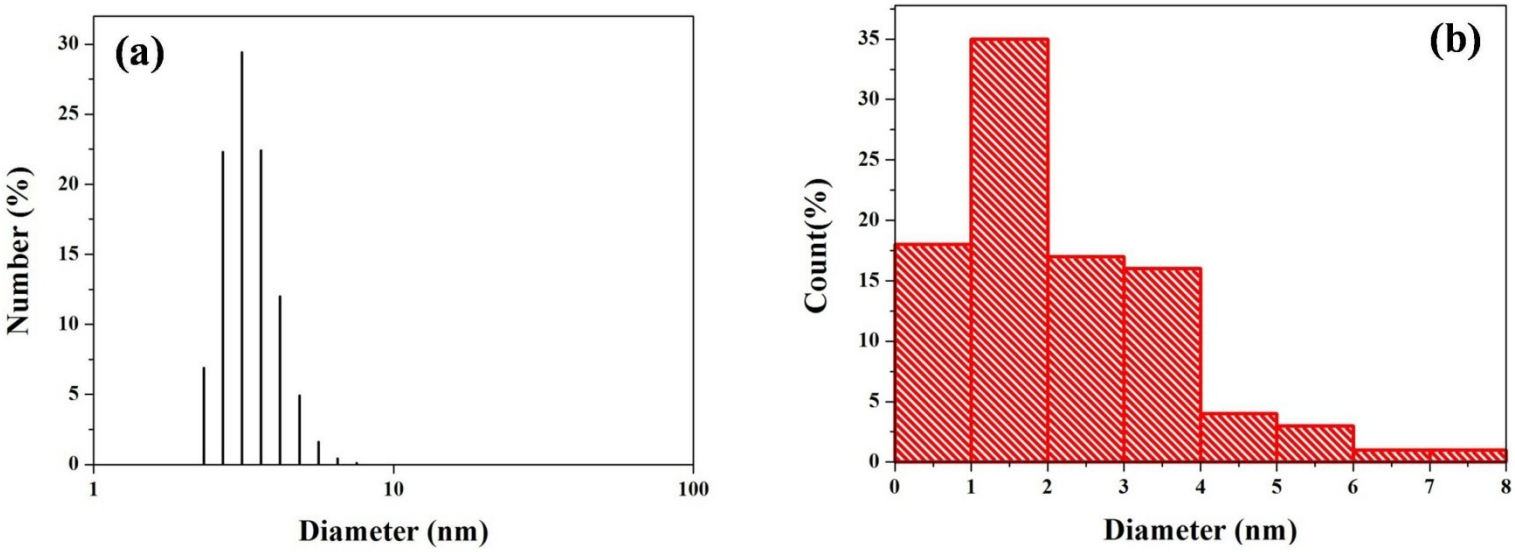

Figure S6. (a) DLS histogram and (b) size distribution histogram obtained from the HR-TEM image of the CD. Both of these histograms show a very good correlation.

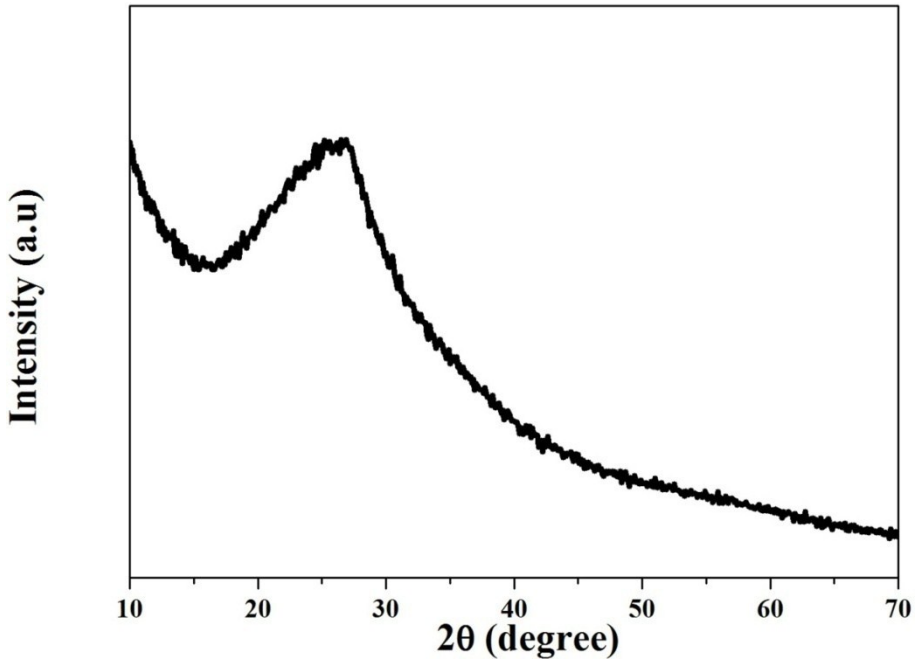

Figure S7. Powder X-ray diffraction (XRD) pattern of the solid CD powder.

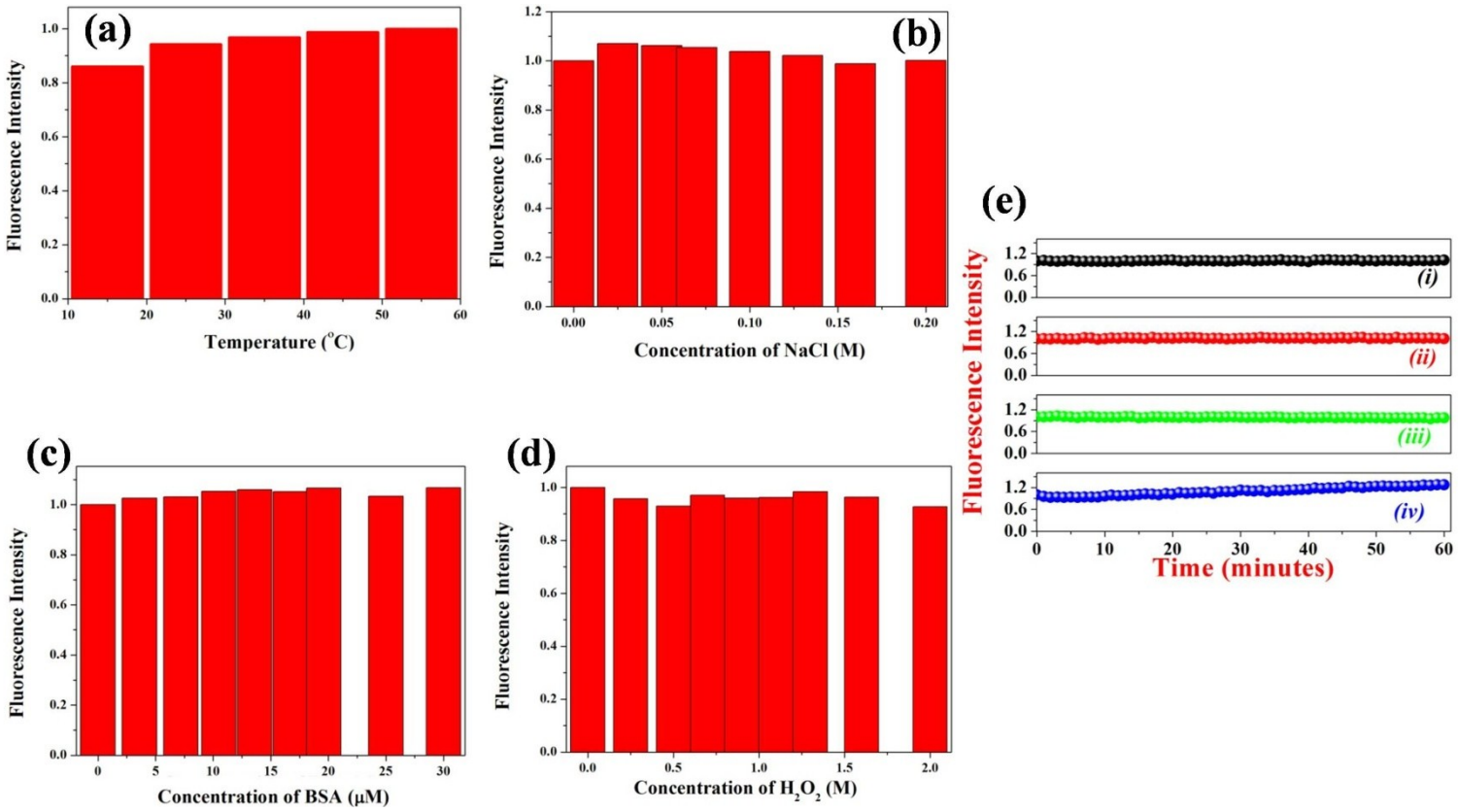

Figure S8. Variation of emission intensity of CD solution with (a) temperature, (b) NaCl, (c) BSA protein and (d) H_2O_2; (e) Effect of the emission intensity of the CD solution with time for 400 nm excitation light (i), NaCl (ii), BSA (iii) and H_2O_2 (iv). All these plots collectively say that the synthesized and dialyzed CD solution is pretty much stable against these foreign parameters.

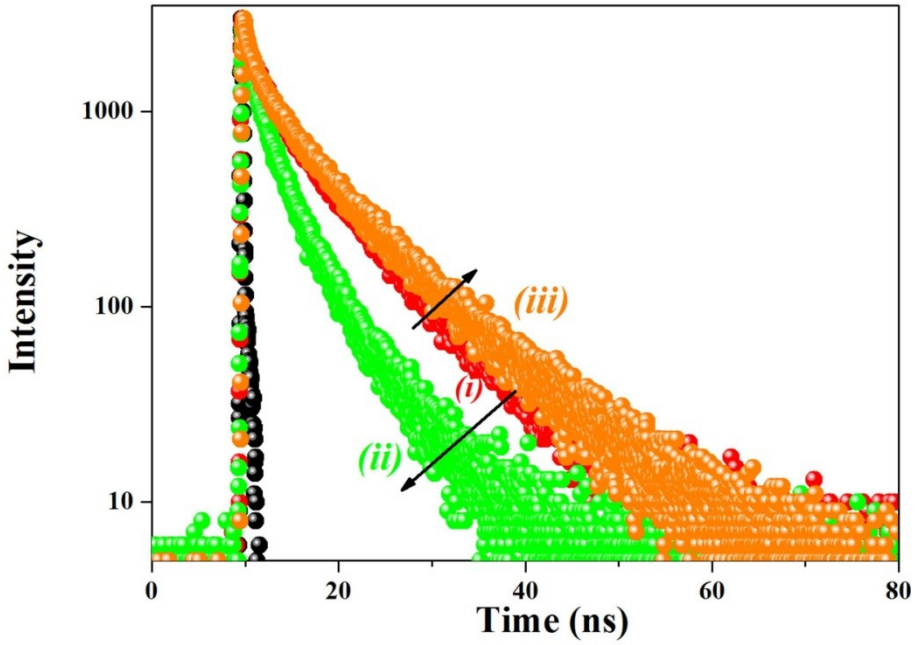

Figure S9. TCSPC lifetime decay profile for the effect of pH on the CD solution (i.e. CD in water (i), CD at pH 2 (ii) and at pH 12 (iii)).

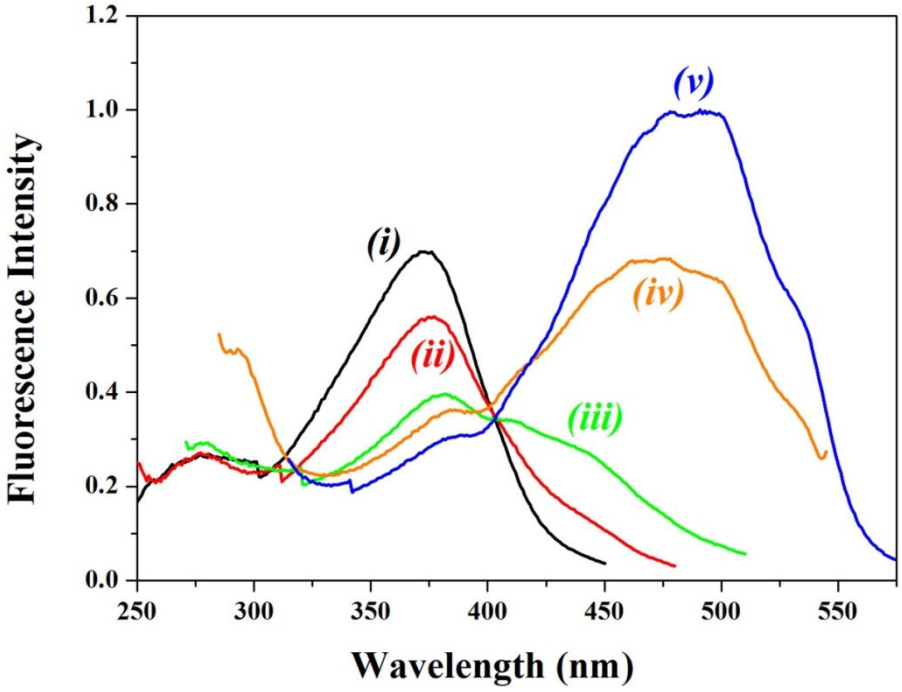

Figure S10: Steady state excitation spectra of CD-Dox WL system for 470 (i), 495 (ii), 525 (iii), 555 (iv) and 592 (v) nm emission wavelengths.

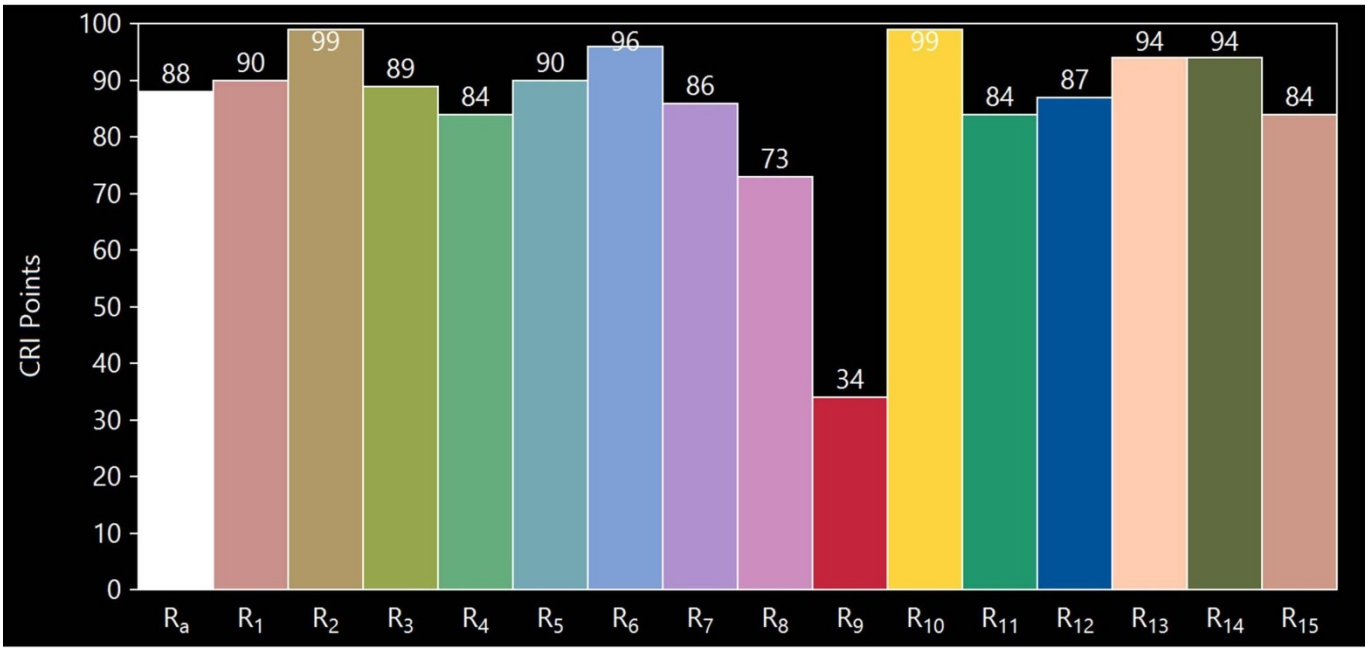

Figure S11. CRI plot (x-axis indicate Munsell code) for CD-Dox WL system. The CRI value (88) is indicated by R_a in the plot and this CRI value is actually the average of all the R_n values.

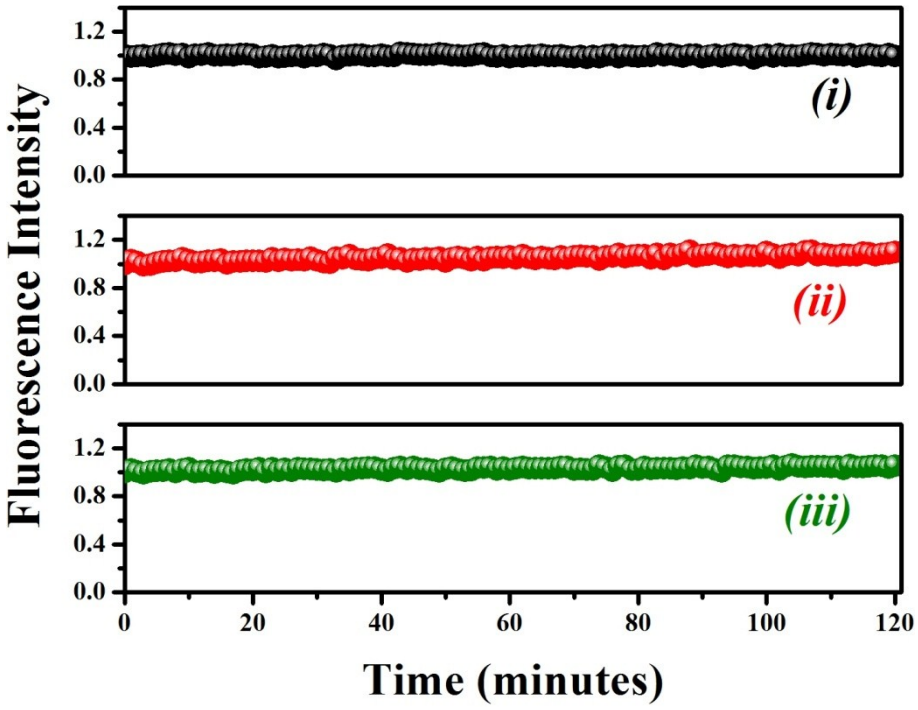

Figure S12. Effect of constant irradiation in steady state fluorimeter (400 nm excitation light) for CD-Dox WL system at (i) 471 nm, (ii) 555 nm and (iii) 592 nm emission wavelengths.

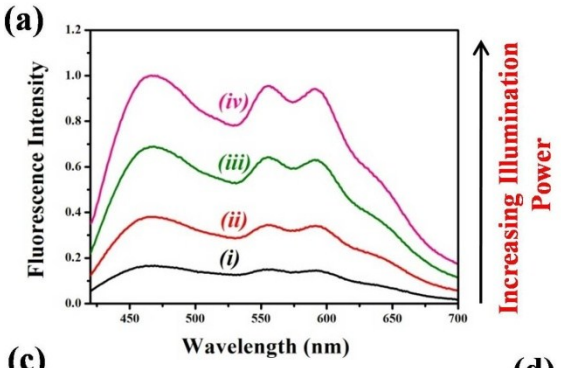

(d)

Excitation Band width (nm)	Emission Band width (nm)	Illumination Power (mW)	Fluorescence Intensity	CIE Coordinate
5	5	1	0.17	(0.32,0.34)
10	5	2	0.38	(0.32,0.34)
15	5	4	0.69	(0.32,0.34)
20	5	8	1.00	(0.32,0.34)

Figure S13. (a) Steady state emission spectra (i to iv indicates spectra with increasing illumination power from 1 to 8 mW), (b) fluorescence intensity histogram, (c) CIE plot and (d) table that summarizes the effect of illumination power on the emission properties of the CD-Dox WL system.

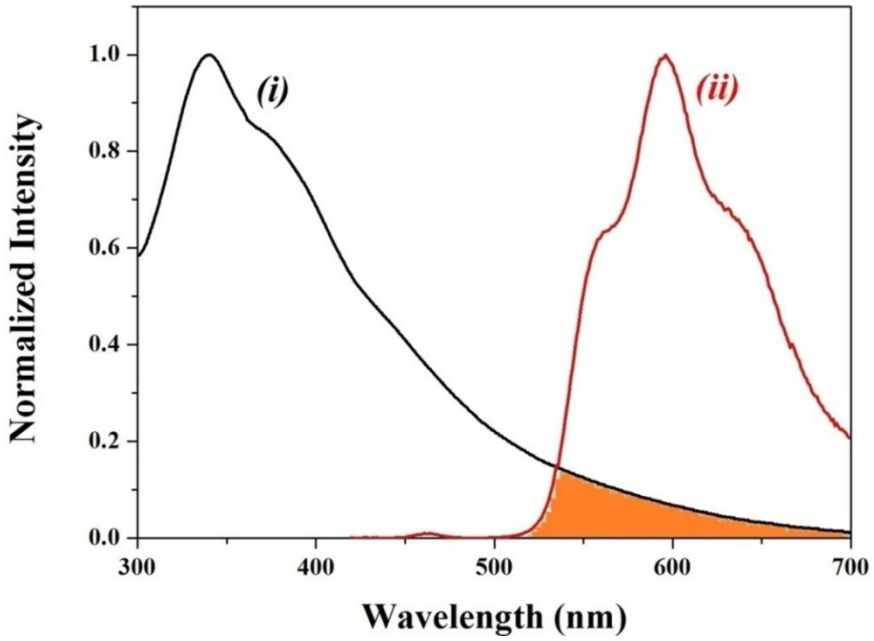

Figure S14. Overlap between absorption spectrum (i) of CD and emission spectrum (ii) of Dox at pH 2.

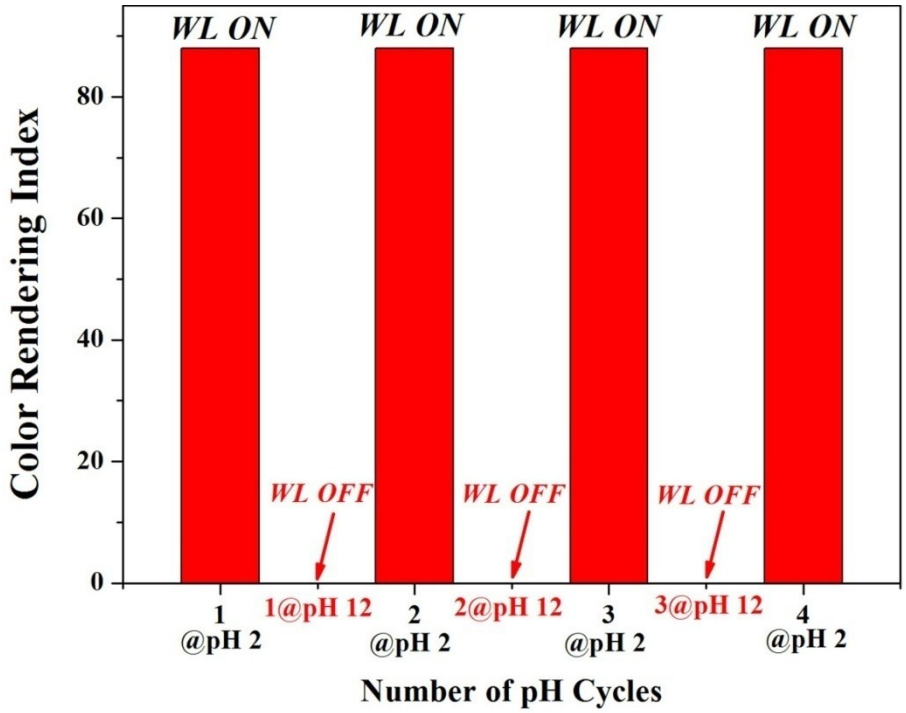

Figure S15. pH reversibility of the CRI values (obtained from the CIE plot) of the CD-Dox WL system.

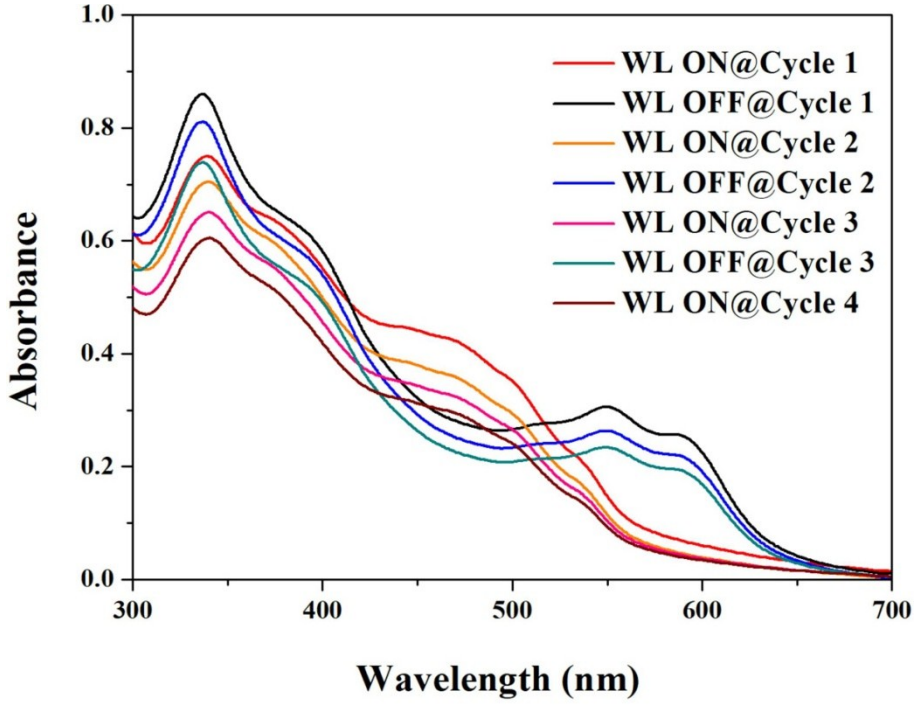

Figure S16. UV-Visible absorption spectra for pH dependent reversible photoswitching of the CD-Dox WL system.

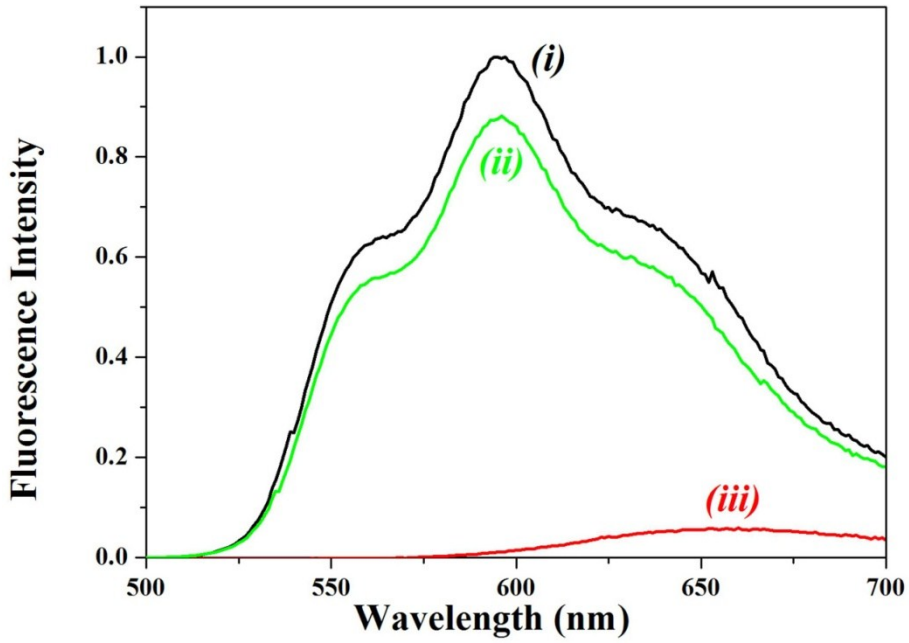

Figure S17. The steady state emission spectra of Dox in water (i), at pH 2 (ii) and at pH 12 (iii).

References.

S1. S. Kundu, A. Pyne, R. Dutta and N. Sarkar, *J. Phys. Chem. C,* 2018, **122**, 6876−6888.

S2. S. Kundu, D. Mukherjee, T. K. Maiti and N. Sarkar, *ACS Appl. Bio Mater,* **DOI: 10.1021/acsabm.9b00107**.